Top Catal (2011) 54:669–684
DOI 10.1007/s11244-011-9685-y

ORIGINAL PAPER

Methanol Adsorption on $V_2O_3(0001)$

Y. Romanyshyn · S. Guimond · D. Göbke · J. M. Sturm · H. Kuhlenbeck · J. Döbler · M. V. Ganduglia-Pirovano · J. Sauer · H.-J. Freund

Published online: 3 May 2011

Abstract Well ordered $V_2O_3(0001)$ layers may be grown on Au(111) surfaces. These films are terminated by a layer of vanadyl groups which may be removed by irradiation with electrons, leading to a surface terminated by vanadium atoms. We present a study of methanol adsorption on vanadyl terminated and vanadium terminated surfaces as well as on weakly reduced surfaces with a limited density of vanadyl oxygen vacancies produced by electron irradiation. Different experimental methods and density functional theory are employed. For vanadyl terminated $V_2O_3(0001)$ only molecular methanol adsorption was found to occur whereas methanol reacts to form formaldehyde, methane, and water on vanadium terminated and on weakly reduced $V_2O_3(0001)$. In both cases a methoxy intermediate was detected on the surface. For weakly reduced surfaces it could be shown that the density of methoxy groups formed after methanol adsorption at low temperature is twice as high as the density of electron induced vanadyl oxygen vacancies on the surface which we attribute to the formation of additional vacancies via the reaction of hydroxy groups to form water which desorbs below room temperature. Density functional theory confirms this picture and identifies a methanol mediated hydrogen transfer path as being responsible for the formation of surface hydroxy groups and water. At higher temperature the methoxy groups react to form methane, formaldehyde, and some more water. The methane formation reaction consumes hydrogen atoms split off from methoxy groups in the course of the formaldehyde production process as well as hydrogen atoms still being on the surface after being produced at low temperature in the course of the methanol → methoxy + H reaction.

Keywords Methanol oxidation · Methanol · Methoxy · Hydroxy · Formaldehyde · $V_2O_3(0001)$

Dedicated to Professor Robert K. Grasselli on the occasion of his 80th birthday

Y. Romanyshyn · S. Guimond · D. Göbke · J. M. Sturm · H. Kuhlenbeck (✉) · H.-J. Freund
Chemical Physics Department, Fritz Haber Institute of the Max Planck Society, Faradayweg 4-6, 14195 Berlin, Germany
e-mail: Kuhlenbeck@FHI-Berlin.MPG.DE

J. Döbler · M. V. Ganduglia-Pirovano · J. Sauer
Department of Chemistry, Humbold-Universität zu Berlin, Unter den Linden 6, 10099 Berlin, Germany

Present Address:
J. M. Sturm
FOM-Institute for Plasma Physics Rijnhuizen, Postbus 1207, 3430 BE Nieuwegein, The Netherlands

Present Address:
J. Döbler
Computer and Media Services, Humbold-Universität zu Berlin, Unter den Linden 6, 10099 Berlin, Germany

Present Address:
M. V. Ganduglia-Pirovano
Institute of Catalysis and Petrochemistry of the Spanish National Research Council, Marie Curie 2, 28049 Madrid, Spain

Present Address:
S. Guimond
Empa, Swiss Federal Laboratories for Materials Science and Technology, Lerchenfeldstr. 5, 9014 St. Gallen, Switzerland

1 Introduction

Vanadium oxides play an important role in catalysis where they act as part of catalysts for different reactions, most of them involving transfer of oxygen atoms [1]. Usually V_2O_5 is

used together with other oxides to improve reactivity and selectivity [2, 3]. The oxy-dehydrogenation of methanol towards formaldehyde ($CH_3OH + O \rightarrow CH_2O + H_2O$) is a reaction which consumes oxygen which may come from the substrate. It is well known that supported vanadia catalyzes methanol conversion [4–6]. Also, studies for ordered thin vanadia films on $CeO_2(111)$ and $TiO_2(110)$ have been performed [7–10]. While it was shown that thin films can be active for the conversion of methanol, the role of the interaction of substrate oxygen with hydrogen atoms from the conversion process was only touched. Farfan-Arribas et al. [11] suggested for the case of methoxy on $TiO_2(110)$ that hydroxy groups and their reaction could modify the defect density on the surface and promote methane formation. Similarly, Mullins et al. suggested for the case of $CeO_2(111)$ on Ru(0001) that reaction induced oxygen vacancies could have an impact on the reactive methanol adsorption [12].

The study presented here aims at shedding some light onto the role of the interaction of hydrogen resulting from methanol conversion with surface oxygen for the case of a $V_2O_3(0001)$ substrate grown on Au(111) [13]. Under standard UHV conditions, this surface is terminated by a layer of vanadyl groups. However, the fully vanadyl terminated surface is inactive and surface defects are necessary to activate the oxide. In order to learn about the role played by vanadyl groups in the methanol conversion reaction the reaction was studied for surfaces where only part of the vanadyl oxygen atoms was removed as well as for surfaces without vanadyl oxygen atoms. To access microscopic details of the reaction, STM (Scanning Tunneling Microscopy) supported by IRAS (Infrared Reflection Absorption Spectroscopy), TPD (Temperature Programmed Desorption), XPS (X-ray Photoelectron Spectroscopy) and NEXAFS (Near Edge X-ray Absorption Fine Structure) as well as DFT (Density Functional Theory) were employed.

2 Experimental

Vibrational spectra were recorded in a chamber equipped with facilities for LEED, TPD, IRAS and HREELS. Infrared absorption spectra were measured with a Bruker IFS 66v/S spectrometer at an incidence angle of the IR light relative to the sample normal of $\sim 85°$. IR spectra were usually obtained by accumulating 600 scans with a resolution of 4 cm^{-1}.

Room temperature STM images were acquired in a system equipped with facilities for STM (Omicron STM 1), XPS, and TPD. Sample heating was performed with a tungsten filament which was mounted behind the sample. It could be used for heating via electron irradiation or via heat radiation in case that no voltage was applied between the filament and the sample. Cooling was possible via a flexible copper braid fixed at the sample holder plate on one side and at a liquid nitrogen evaporator on the other side. With this setup temperatures as low as ~ 100 K could be reached.

For TPD measurements, the sample was placed at a distance of 0.5 mm in front of the nozzle of the pumped housing ('Feulner cup', see ref. [14]) of a quadrupole mass spectrometer (Hiden HAL RC 201). Spectra were recorded with a heating rate 0.5 K/s using a feedback temperature controller (Schlichting Instruments).

XPS and NEXAFS data presented here were measured with light from the UE52 monochromator at the BESSY II electron storage ring in Berlin. High surface sensitivity of XPS was achieved via choosing the photon energy such that the electron kinetic energy of the investigated levels was about 100 eV and by detecting the electrons at an angle of 70° with respect to the surface normal. The electrons were collected with a Scienta SES 200 hemispherical electron energy analyzer. C1s NEXAFS data were recorded with a partial yield detector essentially consisting of a channeltron with two grids mounted in front of its entrance opening. The grid nearer to the channeltron opening was set to a voltage of -60 V in order to reflect low energy electrons and the other grid was set to ground potential. For intensity normalization purposes the spectrum of the adsorbate-covered surface was divided by a spectrum of the non-covered surface.

Methanol with a purity of 99.8% was used for the experiments. It was additionally purified in-situ by repeated freeze/pump/thaw cycles. Details of the gas dosing procedure and the sample and film preparation may be found in ref. [15].

Surface reduction was performed via a tungsten filament put in front of the sample at a distance of some millimeters. Electron energies of 50 and 500 eV were employed and the electron current was in the range of some 10 μA to some mA.

3 Computational Details

Calculations are based on spin DFT and employ a plane wave basis set (400 eV cutoff) as implemented in the VASP code with the PBE functional. The (2×2) $V_2O_3(0001)$ surface was modeled by a four layer slab with a $(3 \times 3 \times 1)$ K-point-mesh. The ($V–O_3–V$) bottom layer was kept fixed at its position in the fully relaxed slab representing the clean surface.

4 Results and Discussion

4.1 Formation of a Methoxy Layer

It has been shown previously with STM, HREELS, IRAS and XPS that the reduction of the vanadyl terminated

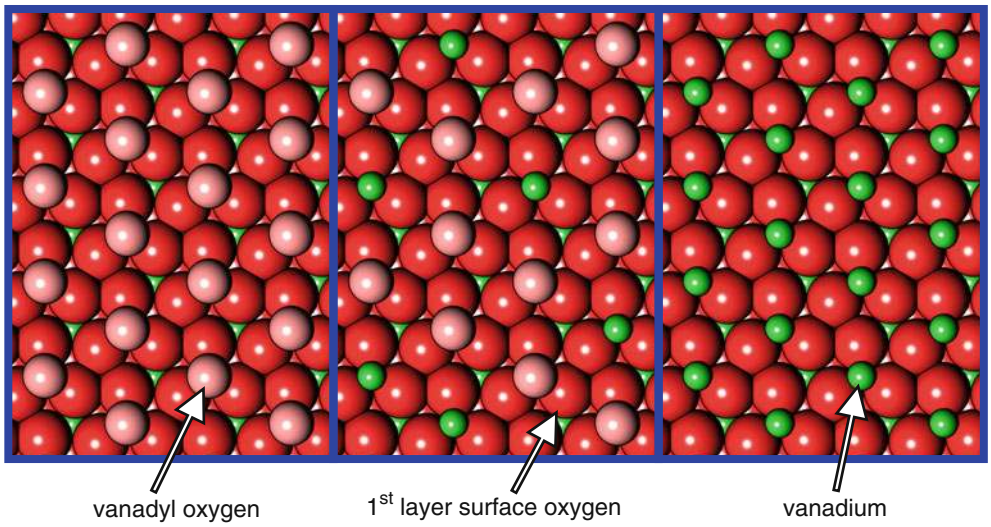

Fig. 1 Top view of the structure of a vanadyl terminated (*left*), a weakly reduced (*center*), and a vanadium terminated $V_2O_3(0001)$ surface (*right*)

surface with an appropriate electron dose leads to a surface terminated by vanadium atoms[13, 15]. Ball models of these surfaces are displayed in Fig. 1 together with a model of a weakly reduced surface. The vanadyl terminated surface exposes oxygen atoms to the vacuum and the vanadium atoms below the oxygen atoms are in a formal 5+ oxidation state whereas the vanadium atoms on the vanadium terminated surface are in a formal 3+ oxidation state which leads to characteristic differences in the V2p XPS spectra [13].

A STM image of the vanadyl terminated surface is shown in Fig. 2. Images of this surface always exhibit some defects which is partially a consequence of the high variability of the vanadium oxidation state. The 3+ oxidation state of the vanadium atoms in V_2O^3 is just an intermediate oxidation state so that defects may form easily by thermal treatment or by an oxygen chemical potential slightly deviating from its optimum value during oxide preparation. Kresse et al. [16] and Schoiswohl et al. [17] have shown that a vanadyl terminated surface may be transformed into a surface with missing vanadyl groups (vanadium+oxygen) by increasing the oxygen chemical potential above the stability regime of the vanadyl terminated surface. Such defects may finally order, giving rise to a $(\sqrt{3} \times \sqrt{3})R30^\circ$ superstructure in the LEED pattern. Using STM and DFT Nilius et al. [18] identified this type of defect as the dominant surface defect on $V_2O_3(0001)$. Another source for defects are contaminations. C1s XPS data (not shown here) demonstrate that the $V_2O_3(0001)$ layers always contain a small amount of carbon. This is probably due to the interaction of metallic vanadium with CO or CO_2 of the residual gas atmosphere during preparation of the oxide layer. We tentatively attribute the fully

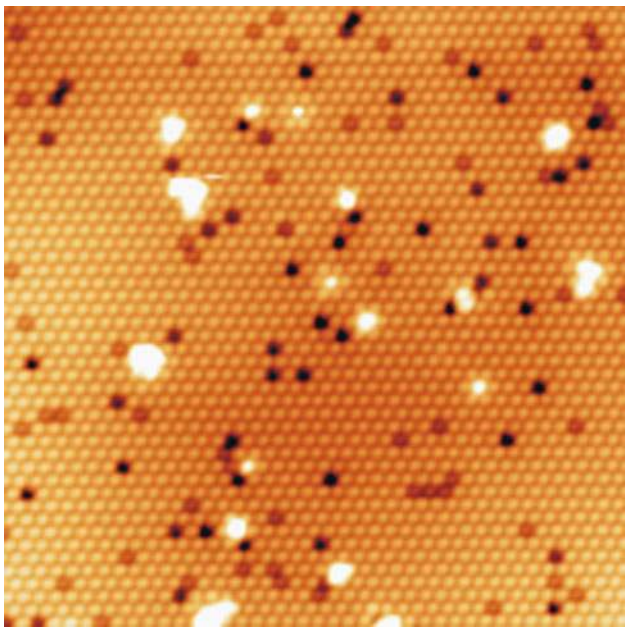

Fig. 2 STM image (constant current topography) of vanadyl terminated $V_2O_3(0001)$. Area: 20×20 nm^2; tunneling conditions: $V = -1.5$ V, $I = 0.2$ nA

dark spots to missing vanadyl groups and the less dark spots to a carbon contamination. The nature of the bright protrusions could not yet be identified. Part of the white protrusions in Fig. 2 appear to consist of a bright intensity at a vanadyl position surrounded by a six-ring of modified vanadyl groups. XPS survey spectra do not show elements other than vanadium, oxygen and a small amount of carbon.

The production of formaldehyde from methanol via oxydehydrogenation consumes oxygen which has to be taken from the substrate surface. To investigate the role of the

vanadyl oxygen atoms in this process we have produced surfaces where only part of the vanadyl oxygen atoms was removed and studied the interaction of methanol with these surfaces.

A set of TPD data is shown in Fig. 3. Formaldehyde forms above 470 K as shown by the data presented in Fig. 3b. According to mass cracking patterns published for methanol and formaldehyde on the NIST WebBook site [19], methanol as well as formaldehyde contribute to the spectrum recorded at mass 29 whereas the spectrum at mass 31 is solely due to methanol. Structures in the spectrum of mass 29, which are not found in the spectrum of mass 31 are due to formaldehyde and structures which are found in both spectra are due to methanol. Comparison of both spectra shows that there are two formaldehyde desorption states between 470 and 620 K.

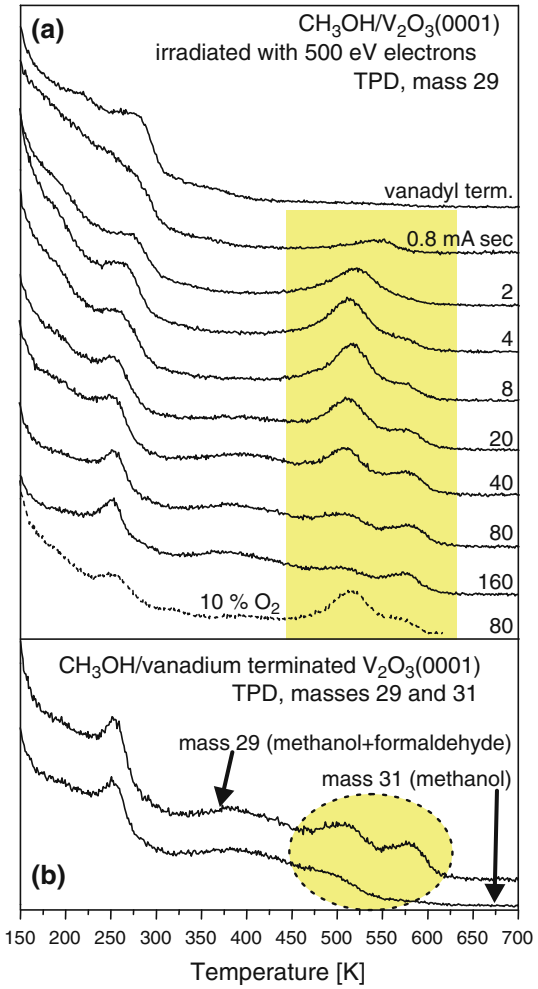

Fig. 3 (**a**) Series of TPD spectra (mass 29: methanol + formaldehyde) of methanol on $V_2O_3(0001)$ as a function of the dose of electrons employed to produce vanadyl oxygen vacancies. (**b**) TPD spectra of masses 29 (methanol + formaldehyde) and 31 (methanol only) of methanol on vanadium terminated $V_2O_3(0001)$. Multilayer amounts of methanol were dosed at 90 K

Figure 3a displays a set of spectra obtained for methanol adsorbed on $V_2O_3(0001)$ exposed to different electron doses. The electrons were employed to produce vanadyl oxygen vacancies in the vanadyl layer. The amount of desorbing formaldehyde clearly depends on the degree of surface reduction with a maximum of the low-temperature peak at an electron dose of 4–8 mC whereas the intensity of the high-temperature peak increases with increasing electron dose. An electron dose of about 80 mC removes more or less all vanadyl oxygen atoms as concluded from STM data (not shown here) so that a dose of 4–8 mC produces a surface where only a part of the vanadyl oxygen atoms is removed. From this we conclude that the low-temperature formaldehyde desorption state results from a reaction involving vanadyl oxygen atoms and the reaction leading to the high-temperature desorption state occurs on surface areas without vanadyl oxygen atoms. At the bottom of Fig. 3a a TPD spectrum of a mixture of oxygen (10%) and methanol (90%) adsorbed onto a surface without vanadyl oxygen atoms (vanadium terminated) is shown. It is very similar to the spectra obtained for methanol on surfaces with part of the vanadyl oxygen atoms removed, demonstrating that co-adsorbed oxygen acts the same way as vanadyl oxygen atoms do, probably since oxygen adsorption onto vanadium terminated $V_2O_3(0001)$ leads to the formation of vanadyl groups above $\sim$200K [15]. The top spectrum in Fig. 3a finally shows that formaldehyde does not form on a vanadyl terminated surface which means that the defects visible in Fig. 2 are not active for formaldehyde formation.

The mechanism of methoxy formation was investigated with STM for low degrees of surface reduction as a function of the dose of reducing electrons. A set of STM data for two different electron doses (E_{kin} = 50 eV) is shown in Fig. 4 which displays (from left to right) images recorded before reduction, after reduction, and after dosage of methanol at 90 K followed by a flash at 400 K in order to remove molecularly adsorbed methanol. Methoxy groups and vacancies are clearly identifiable. The methoxy groups in the right column of Fig. 4 are not fully randomly distributed on the surface in that they seem to partly line up in the lower image. It could be the case that there is some kind of line defect with an increased sensitivity towards reduction by electron irradiation.

As discussed before, the defects found on the vanadyl terminated surface are not active for formaldehyde formation which is the reason for a significant density of unoccupied defects remaining on the surface after methanol dosage. These defects are inactive since both types of defects (missing vanadyl group and carbon contamination) do not represent reasonable bonding partners for the methoxy groups. Methoxy groups bond to defects where vanadium atoms are available and accessible which is the case for defects formed by electron irradiation.

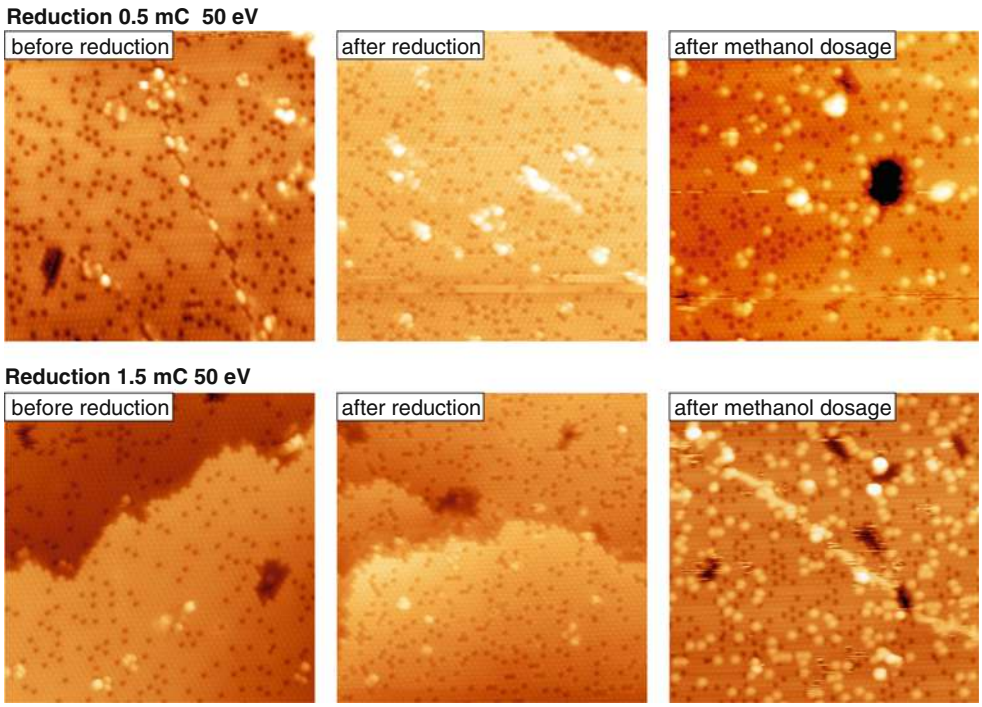

Fig. 4 STM data documenting the formation of methoxy from methanol on partially reduced $V_2O_3(0001)$. Surfaces with two different densities of vanadyl oxygen vacancies were prepared by irradiation with 0.5 and 1.5 mC of 50 eV electrons, respectively. The data were recorded at room temperature in CCT (constant current topography) mode with a tunnelling voltage of −1.5 V and a current of 0.2 nA. The images show an area with a width of 25 nm

These STM images were subjected to a quantitative evaluation of the relation between the density of methoxy groups and the number of defects produced by electron irradiation. The different types of defects could not be differentiated with STM so that we determined the increase of the defect density due to electron irradiation by subtracting the density of surface defects before electron irradiation from the density of defects after electron irradiation. The result of the evaluation of the STM data is shown in Fig. 5. We employed electrons with two different energies (50 and 500 eV) in order to check whether the result depends on the electron energy. As can be seen from Fig. 5, *one* surface defect (a site where the oxygen atom of a vanadyl group is removed) leads to the formation of about *two* methoxy groups. This relationship is very obvious for the data shown in the lower panel (500 eV electron energy) whereas for the data in the upper panel (50 eV electron energy) the ratio appears to be slightly different. Whether this has physical reasons or whether this is related to experimental uncertainties is currently not clear. As expected, the electron energy is a critical parameter for the density of defects produced on the surface: electrons with a kinetic energy of 500 eV produce ~2.5 times more defects than electrons with a kinetic energy of 50 eV. In view of the larger inelastic mean free path (IMFP) of electrons with a kinetic energy of 500 eV as compared to electrons with a kinetic energy of 50 eV it may be assumed that the action of secondary electrons is responsible for the higher surface defect density produced by electrons with a kinetic energy of 500 eV.

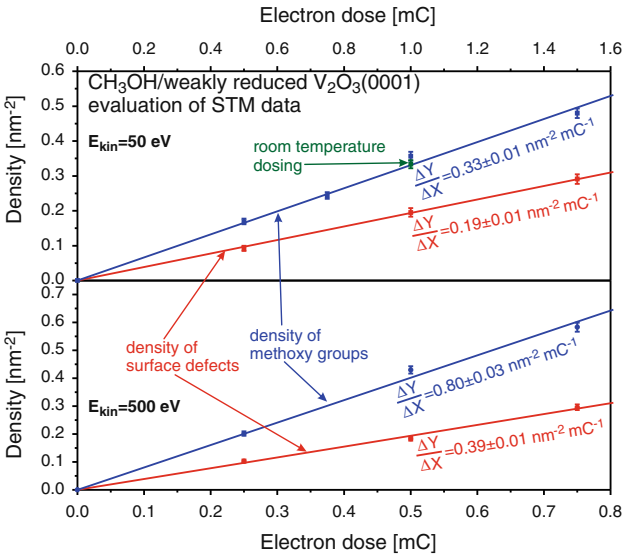

Fig. 5 Density of defects induced by electron irradiation as a function of the electron dose for two electron energies (E = 50, 500 eV) and the corresponding density of methoxy groups after methanol dosage at 90 K followed by a flash to 400 K as obtained from STM images

The somewhat unexpected result that the density of methoxy groups is two times higher than the density of defects produced by electron irradiation may be explained by assuming that additional surface defects are formed by the reaction of hydroxy groups on the surface. The first step of the reaction probably occurs already when methanol is adsorbed at 85 K. Here *n* surface defects (vanadium sites,

denoted by 'V' in the following) and n surface vanadyl groups ('VO') interact with n methanol molecules to form n methoxy ('CH_3OV') and n hydroxy groups ('VOH'):

$$n\mathrm{CH_3OH} + n\mathrm{V} + n\mathrm{VO} \rightarrow n\mathrm{CH_3OV} + n\mathrm{VOH} \quad (1)$$

When the surface is warmed up, the hydroxy groups react in pairs to form water which leads to a water desorption peak at $\sim$270 K (see TPD data in Fig. 6). In addition to water, this reaction produces vanadyl and vanadium sites [reaction step (2)] which react with molecularly adsorbed methanol to form additional methoxy and hydroxy groups [reaction step (3)]:

$$n\mathrm{VOH} \rightarrow \frac{n}{2}\mathrm{H_2O} + \frac{n}{2}\mathrm{VO} + \frac{n}{2}\mathrm{V} \quad (2)$$

$$\frac{n}{2}\mathrm{CH_3OH} + \frac{n}{2}\mathrm{V} + \frac{n}{2}\mathrm{VO} \rightarrow \frac{n}{2}\mathrm{CH_3OV} + \frac{n}{2}\mathrm{VOH} \quad (3)$$

Figure 6 exhibits a methanol desorption peak at 288 K. We always found that methanol desorption leads to the occurrence of intensity in the water spectrum which is also the case in Fig. 6. However, water is not a component of the mass cracking pattern of methanol [19] so that we assume that the water is the result of an exchange reaction at the walls of the mass spectrometer housing. The occurrence of the methanol desorption state at 288 K means that methanol is still available at the temperature where the hydroxy groups react (270 K) which is required for reaction step (3). Reaction step (4) again produces vanadyl and vanadium sites which react with methanol to form more methoxy and hydroxy groups [reaction step (5)]:

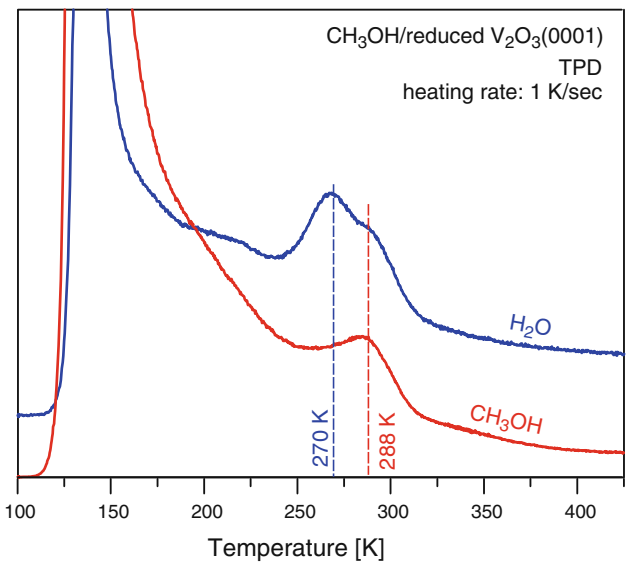

Fig. 6 TPD traces (mass 18: H_2O and mass 31: CH_3OH) of methanol adsorbed at 90 K onto moderately reduced (electron dose: 8 mC) $V_2O_3(0001)$

$$\frac{n}{2}\mathrm{VOH} \rightarrow \frac{n}{4}\mathrm{H_2O} + \frac{n}{4}\mathrm{VO} + \frac{n}{4}\mathrm{V} \quad (4)$$

$$\frac{n}{4}\mathrm{CH_3OH} + \frac{n}{4}\mathrm{V} + \frac{n}{4}\mathrm{VO} \rightarrow \frac{n}{4}\mathrm{CH_3OV} + \frac{n}{4}\mathrm{VOH} \quad (5)$$

The increase of the methoxy coverage is accompanied by an increase of the methoxy C–O vibrational intensity when the temperature is increased from 240 to 270 K (see Fig. 7). This self-limiting chain reaction goes on until the number of produced defect sites approaches zero. The total number of methoxy groups finally formed is:

$$n\mathrm{CH_3OV} + \frac{n}{2}\mathrm{CH_3OV} + \frac{n}{4}\mathrm{CH_3OV} + \frac{n}{8}\mathrm{CH_3OV} + \cdots = 2n\mathrm{CH_3OV} \quad (6)$$

This means that the number of methoxy groups is twice as large as the number of surface defects giving rise to their formation which is in full agreement with the data displayed in Fig. 5. The reaction is schematically represented in Fig. 8 for $n = 6$. The description presented above considers only the reaction of hydroxy groups to form water, but ignores the reaction of methoxy groups with hydroxy groups to form methanol. While this reaction may occur (we do not have evidence in favor or disfavor of this) it would probably not change the final result since the resulting V + VO pair would react with methanol to yield a methoxy and a hydroxy group.

Figure 5 also shows a data point for room temperature dosing in the upper panel. In this case the surface was exposed to 4×10^{-7} of methanol at room temperature for five minutes. Obviously the result for dosing at room temperature is the same as for low temperature dosing indicating that the processes occurring during exposure of the sample to methanol at room temperature and those

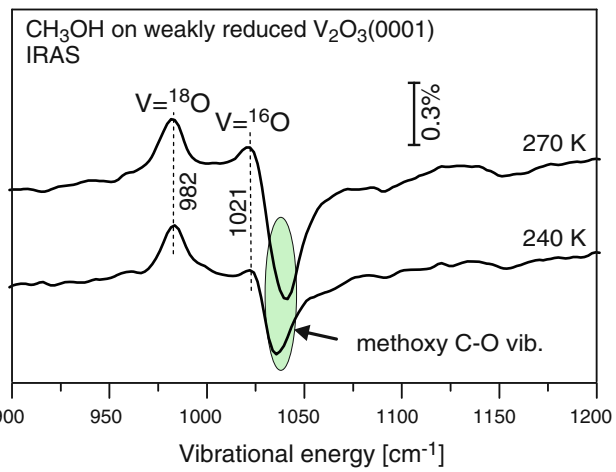

Fig. 7 IRAS spectra of methanol adsorbed on moderately reduced (electron dose: 8 mC) $V_2O_3(0001)$. Methanol was dosed at 90 K and the spectra were recorded after warming up to 240 and 270 K, respectively

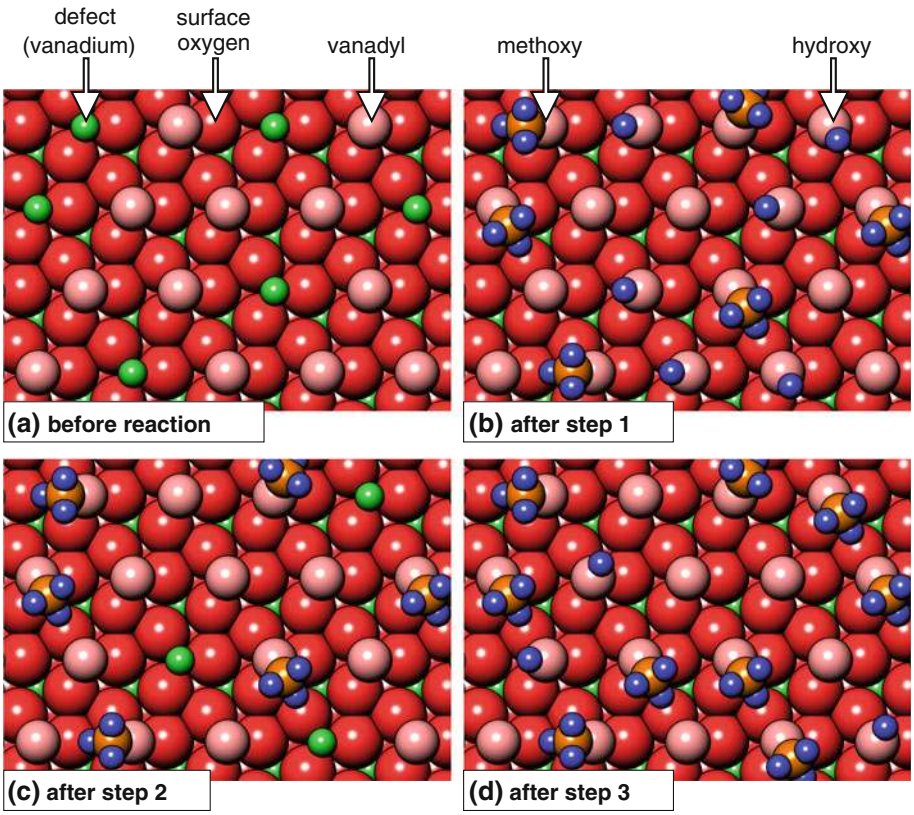

Fig. 8 Graphical Illustration of the formation of a methoxy layer on $V_2O_3(0001)$ according ro reaction steps 1–3

occurring in the methanol layer while it is warmed up are similar. The main difference may be that the defects produced by water formation during room temperature dosing have to react with molecules from the gas phase (which may be short-time trapped at the surface) whereas in the case of low temperature dosing chemisorbed methanol molecules are available. Another results of the room temperature experiment was that high methanol doses do not lead to more methoxy groups which is another indication that the density of surface defects and not the methanol dose limits the methoxy coverage.

Figure 9 exhibits IRAS data for methanol on partially reduced $V_2O_3(0001)$ as a function of the annealing temperature. After dosing methanol at 88 K vibrational features of a methanol multilayer get visible. These features are gradually replaced by a mixture of methoxy and monolayer methanol features until at temperatures of above 270 K methoxy prevails, being visible until about 570 K. The assignment of the vibrational bands as given in Fig. 9 is based on data published for adsorbed methanol [20, 21] and methoxy [22–24].

At the bottom of Fig. 9 spectra of the fully vanadyl terminated surface are shown to indicate the presence of ^{18}O and ^{16}O which give rise to vanadyl induced vibrations at 997 cm^{-1} [$\nu(V = {}^{18}O)$] and 1,034 cm^{-1} [$\nu(V = {}^{16}O)$]. The two bands exhibit comparable intensities although the layer was grown with ^{18}O. There is probably also a ^{16}O contamination which could stem from the interaction of the oxide with the residual gas atmosphere. We assume that vibrational dipole coupling shifts intensity from the low energy band to the high energy band [25–28]. This can be a significant effect [27] so that a small concentration of ^{16}O can produce an intense vibrational absorption line as in Fig. 9. At the bottom of Fig. 9 the spectrum of the partially reduced oxide layer is shown, exhibiting shifted vanadyl vibrations. The shift is likely due to the reduced density of oscillators on the surface which reduces the vibrational dipole coupling, leading to a downward shift of the vibrational frequencies [25–28]. Upon methanol adsorption the intensity of the vanadyl vibrations decreases as evidenced by the features with positive intensity at 982–984 and 1,023–1,025 cm^{-1} in the spectra recorded after methanol adsorption. We attribute this to the transformation of vanadyl groups into hydroxy groups in reaction step (1).

At 240 K hydroxy groups and molecular methanol are on the surface together with the methoxy groups. Warming up to 270 K and higher first removes the hydroxy groups and then methanol disappears. The removal of the hydroxy groups is accompanied by an increase of the methoxy coverage which leads to an increase of the intensity of all methoxy bands. At about this temperature the bands at 1,460, 1,059–1,062, 1,034, 2,852, 2,947, and 2,960 cm^{-1} in Fig. 9 vanish which indicates that this change is related to the disappearance of co-adsorbed methanol molecules and the hydroxy groups.

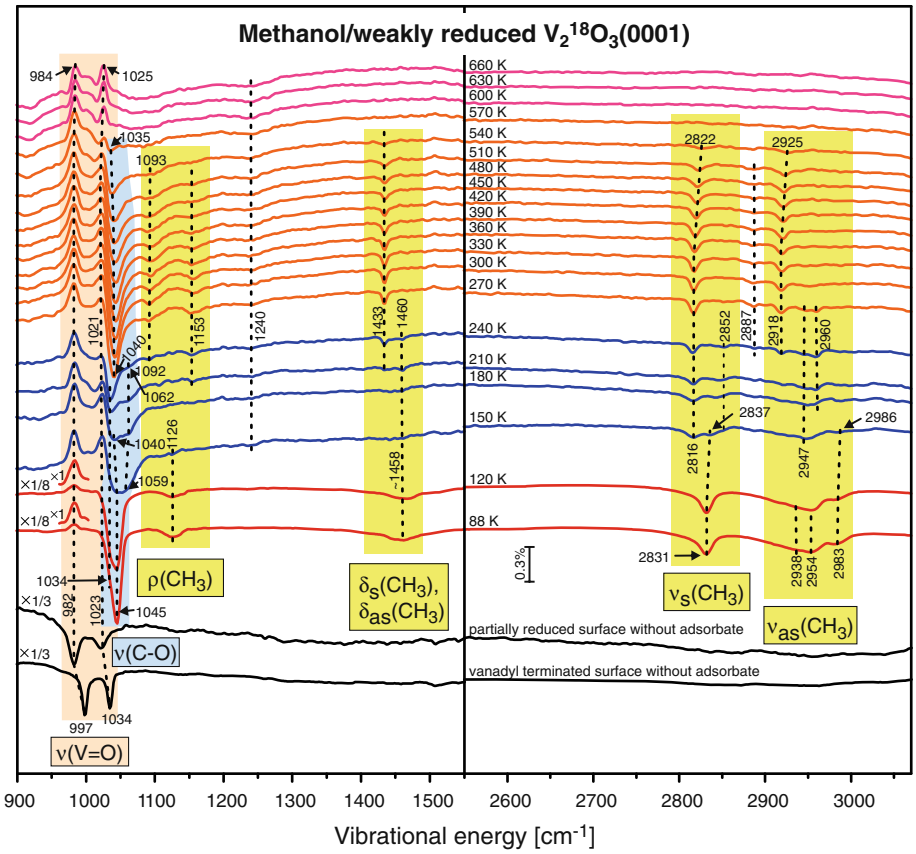

Fig. 9 Infrared absorption spectra of CH_3OH adsorbed on partially reduced $V_2O_3(0001)$ as a function of temperature. Methanol was adsorbed at 88 K. Before recording a spectrum the sample was shortly flashed to the temperature given at the respective spectrum and the spectra were recorded after the sample had cooled down to below 100 K. The $V_2O_3(0001)$ substrate contained a mixture of ^{18}O and ^{16}O. All spectra are referenced to the spectrum of the partially reduced surface recorded before methanol adsorption except for the two spectra at the bottom which were referenced to the spectrum of the fully reduced surface. *Black* non-covered surfaces; *red* methanol multilayer; *blue* mixture of methanol, hydroxy, and methoxy before water formation; *orange* methoxy after water desorption; *pink* after formaldehyde desorption

Thus these vibrations are either vibrations of the methanol molecules or of the methoxy groups which shift when the co-adsorbed methanol molecules and the hydroxy groups disappear.

A band at $\sim$1,240 cm^{-1} is also found in IR spectra of water and CO_2 on $V_2O_3(0001)$ (not shown here). We assume that it is related to an overtone of a substrate phonon which is found at $\sim$650 cm^{-1} [13].

The behavior of the vanadyl intensity is somewhat different in the case of the fully reduced surface (see Fig. 10). Positive intensity (indicating removal) is found at 1,021 cm^{-1} whereas negative intensity (indicating formation) is found at 968–972 cm^{-1} in the spectra at the top. The latter line may be attributed to the diffusion of ^{18}O at high temperature from the bulk to the surface (this may also play a role for the partially reduced surface) whereas the presence of the line at 1,021 cm^{-1} is related to the decrease of V = ^{16}O vibrational intensity. This indicates that V = ^{16}O groups were formed on the fully reduced surface (reference spectrum for the IRAS data in Fig. 10) due to adsorption of gases from the residual gas atmosphere [adsorbed CO_2 interacts strongly with the fully reduced surface and leads to the formation of vanadyl groups (not shown here)]. Similar to the case of the partially reduced surface (see Fig. 9) these ^{16}O vanadyl groups were consumed for hydroxy and water formation in the course of the interaction of the surface with methanol which is probably the reason for the positive intensity at 1,021 cm^{-1}.

The methoxy formation mechanism in the case of the fully reduced surface is somewhat less well documented in that supporting STM data are not available, but some information may be derived from the existing TPD, IRAS and PES data. As indicated by the TPD data displayed in Fig. 11b, water desorbs with a peak maximum at $\sim$240 K. At about this temperature the intensity of the methoxy C–O vibration in the infrared data displayed in Fig. 10 increases significantly indicating that a reaction mechanism as described above for weakly reduced $V_2O_3(0001)$ might also be operative for the fully reduced surface. The reaction consumes surface oxygen for the formation of water which probably comes from the first oxygen layer of the $V_2O_3(0001)$ surface. The somewhat different water desorption temperature (compared to the case of the weakly reduced surface) indicates that in the current case different surface oxygen atoms are involved.

4.2 Electron Spectroscopy Data

The O1s XPS data displayed in Fig. 12b are in agreement with the discussed reaction scheme. At 530.2–530.3 eV the emission of substrate O1s level is found and the methanol O1s peak is located at 533.3–533.9 eV [12]. The methanol

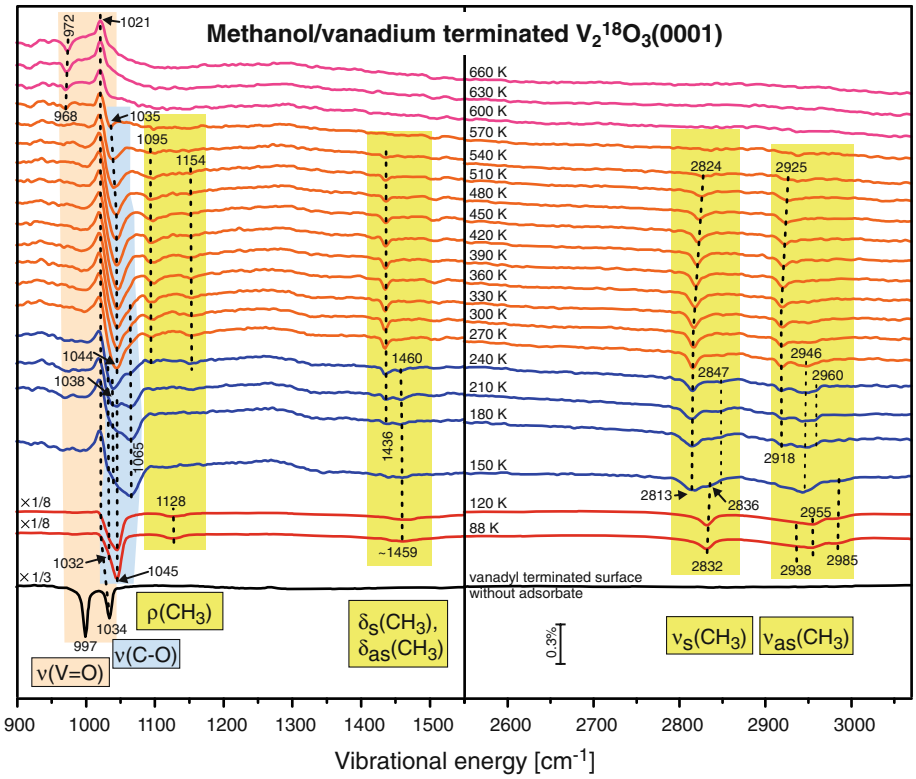

Fig. 10 Infrared absorption spectra of CH_3OH adsorbed on vanadium terminated $V_2O_3(0001)$ as a function of temperature. Methanol was adsorbed at 88 K. Before recording a spectrum the sample was shortly flashed to the temperature given at the respective spectrum and the spectra were recorded after the sample had cooled down to below 100 K. The $V_2O_3(0001)$ substrate contained a mixture of ^{18}O and ^{16}O. All spectra are referenced to the spectrum of the fully reduced surface recorded before methanol adsorption. *Color code* as in Fig. 9

level in the spectrum at the bottom is attributed to multilayer methanol which evaporates upon annealing at 225 K. The remaining methanol has direct contact with the substrate and/or the methoxy groups and is characterized by a slightly shifted O1s level (533.3 eV). At 531.4–531.7 eV emission of methoxy and hydroxy groups shows up [12]. Below the water desorption temperature (240 K) the level is located at 531.4 eV and above this temperature it is found at 531.7 eV with about the same intensity. The energy shift indicates that something has changed which probably is the formation of additional methoxy groups and the formation of water from hydroxy groups. The intensity of this peak does not change very much since it represents the O1s intensity of the methoxy groups as well as of the hydroxy groups. As indicated by reaction steps 1 and 6 the sum of the number of methoxy and hydroxy groups is the same below and above the water desorption temperature. At 400 K the intensity of the methanol peak has essentially vanished as expected. The small remaining intensity may be attributed to adsorption of methanol from the residual gas atmosphere which contained some methanol after dosing in case of the XPS chamber. Since the data were recorded at a sample temperature below 200 K this could adsorb molecularly. Annealing at 550 K removes most of the methoxy groups and therefore only a weak shoulder remains. A point to note is the appearance of the $V2p_{3/2}$ level. This level does not exhibit a shoulder at higher binding energy like the spectrum of the vanadyl terminated surface (see arrows). As has been shown previously, the shoulder is indicative of a vanadyl terminated surface [13] and its absence shows that notable re-oxidation of the surface did not take place.

The C1s data shown in Fig. 12a exhibit the C1s peak of a methanol multilayer (bottom spectra) at 287.9 eV which is not too different from the C1s binding energy observed for methanol on $CeO_2(111)$ by Mullins et al. [12]. Annealing at 225 K removes the methanol molecules adsorbed in higher layers and a mixture of methoxy and methanol molecules remains on the surface. In the C1s spectra these species can not be separated (in the O1s spectra the existence of two species is obvious) and the binding energy shifts to a somewhat lower value in rough agreement with results for methoxy on $CeO_2(111)$ [12] and $TiO_2(110)$ [11]. Warming up to 400 K shifts the C1s level by 300 meV down do 286.7 eV. This shift may be attributed to the missing methanol intensity as well as to the disappearance of the methoxy–methanol interaction. Annealing at 550 K removes most methoxy groups from the surface and at 700 K all groups are gone, in agreement with the TPD and infrared data. The level at 289.7 eV is attributed to a CO_2 induced contamination like carbonate.

C1s NEXAFS data of methanol on fully reduced $V_2O_3(0001)$ were recorded after annealing at different temperatures for three different light incidence angles α (Fig. 13). The spectra are similar to those observed by Mullins et al. for methanol and methoxy on cerium oxide

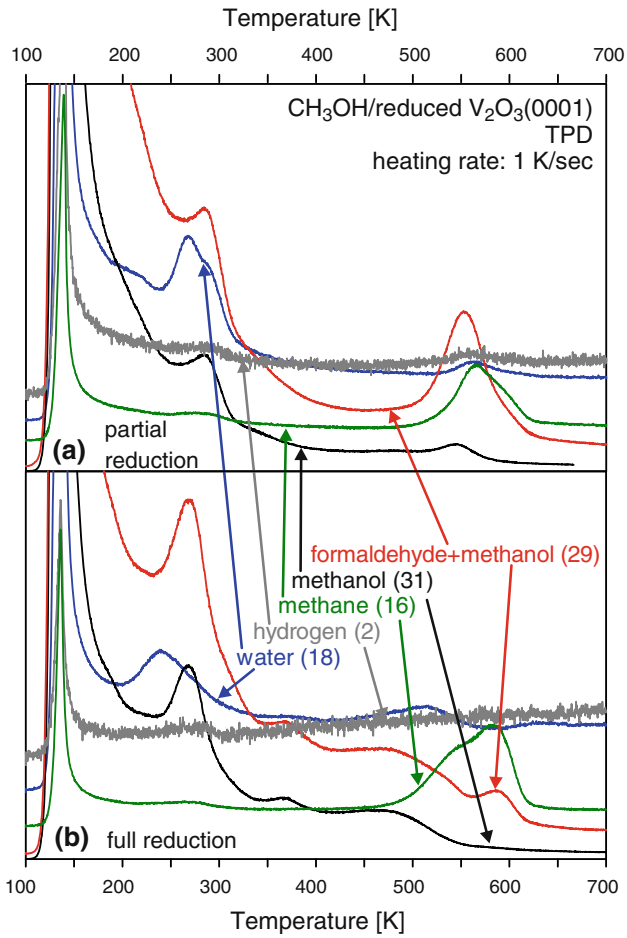

Fig. 11 Thermal desorption spectra of methanol on partially and fully reduced $V_2O_3(0001)$. (**a**) Shows data for a partially reduced surface (electron dose: 2 mC) and (**b**) displays data for a fully reduced surface (electron dose: 80 mC). Methanol was adsorbed in multilayer amounts at 90 K

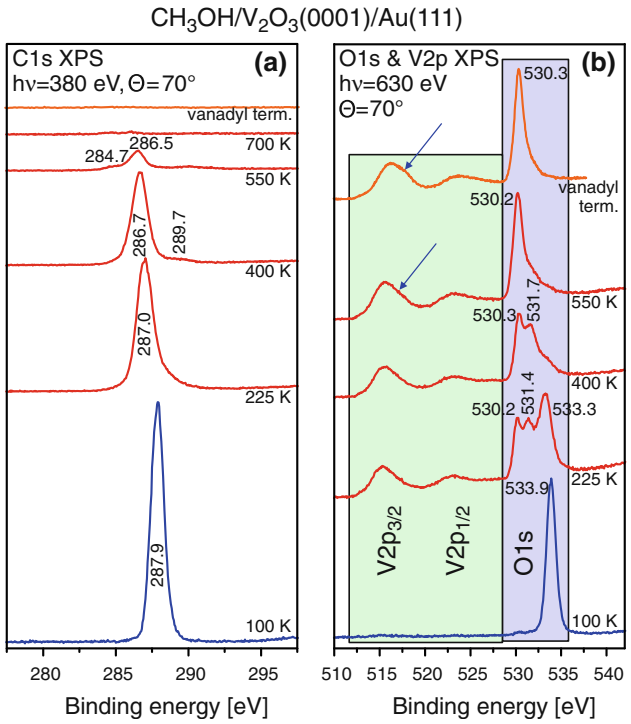

Fig. 12 XPS data of methanol on fully reduced $V_2O_3(0001)$ recorded at an exit angle of 70° relative to the surface normal as a function of temperature. Multilayer amounts of methanol were admitted at 100 K and the spectra were recorded after annealing at the given temperatures. The regimes where the O1s and V2p intensities are located are marked by colored backgrounds in (**b**)

[12]. However, in the latter case the angular dependence was not investigated.

The spectra shown in Fig. 13 for a temperature of 85 K relate to a methanol multilayer, the spectra obtained after annealing at 225 K are from a mixture of methoxy groups and molecular methanol molecules and the spectra recorded after annealing at 400 K are spectra of pure methoxy. The near edge region between 288 and 290 eV is dominated by two resonances (R_1 and R_2 in Fig. 13) and at ~293 eV a somewhat broader resonance (R_3) is seen in the spectra recorded after annealing at 225 and 400 K. In the spectra recorded after annealing at 400 K this state can not be assigned unambiguously. Here intensity normalization problems probably play a role. The photon monochromator used for these measurements had a deep and structured intensity minimum in the C1s absorption edge regime which was somewhat time-dependent. Due to the time-dependence a perfect intensity normalization could not be achieved and especially in the range of the excitations above 292 eV uncertainties do exist. This applies in particular to the set of data recorded after annealing at 400 K since in this case the signal intensities are low.

The spectra of the methanol multilayer (bottom) depend only weakly on the light incidence angle whereas the spectra recorded after annealing at 225 and 400 K exhibit a somewhat more pronounced polarization dependence which is indicative of a preferential molecular orientation. For perpendicular light incidence ($\alpha = 0°$) resonance R_2 is more intense than R_1 whereas for grazing light incidence ($\alpha = 80°$) R_1 prevails. The somewhat weaker but still clearly detectable polarization dependence of the relative intensities of these two resonances in the case of the methanol multilayer (bottom spectra) implies that also in this case a preferential orientation does exist which may be attributed to the presence of the oxide surface and also to the possible existence of a preferential orientation at the surface of the multilayer. The intensity of R_3 in the spectra of the multilayer and the layer obtained after annealing at 225 K is also dependent on the light polarization in that it is higher in the spectra obtained for grazing light incidence. According to Prince et al. [29] and Plashkevych et al. [30] the C1s spectra of methyl groups do not depend much on the nature of their bonding partners and therefore one may

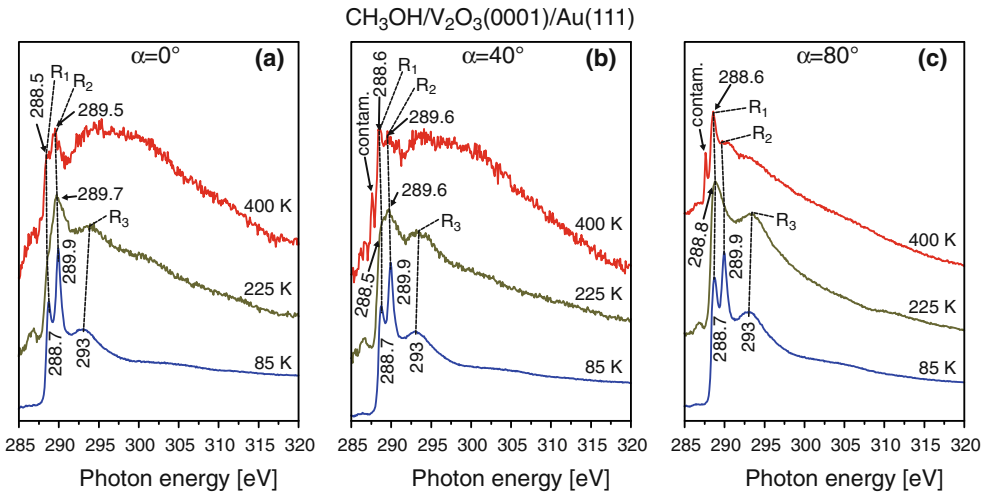

Fig. 13 NEXAFS data of methanol on fully reduced $V_2O_3(0001)$ recorded with a partial yield detector as a function of temperature for three different light incidence angles α which are given relative to the surface normal. Multilayer amounts of methanol were admitted at 85 K and the spectra were recorded after annealing at the given temperatures. The absorption at ~287.5 eV is probably due to a CO contamination (being strongly tilted with respect to the surface normal according to the data) as tested in a blank experiment

assume that the C1s spectra of methanol and methoxy are similar as is also suggested by the spectra presented in Fig. 13.

Prince et al. [29, 31] published a C1s NEXAFS spectrum of gas phase methanol which fits well to the measured methanol multilayer spectra (bottom spectra in Fig. 13) after application of a 0.5 eV shift to the energy scale. According to reference 29 the R_1 and R_2 resonances are due to 3s and 3p type molecular Rydberg states, respectively, partially including vibrational excitations. R_3 is assigned to a multitude of higher Rydberg states coupled with vibrations. We note that according to common belief Rydberg transitions are quenched for adsorbates on metal substrates [32, 33]. However, this is an unproven rule and it may be expected that it is relaxed for oxide surfaces due to their lower or negligible electron density near to the Fermi edge and the rule may also be relaxed if the excitation is located in a part of the molecule which is somewhat distant from the surface.

A NEXAFS study of methoxy on Cu(100) was published by Lindner et al. [34]. R_3 was assigned to a C–O σ^* resonance, in agreement with assignments published by Outka et al. [35] and Ishii and Hitchcock [36] for methanol multilayers. Lindner et al. found a significant dependence of the R_3 intensity on the light incidence angle which led them to the conclusion that the C–O molecular axis is oriented parallel to the surface normal in the investigated case. The clear polarization dependence indicates that an assignment of this resonance to a multitude of different levels with different symmetries as indicated by a comparison with the methanol gas phase spectrum published by Prince et al. [29, 31] is probably not appropriate. Below 290 eV only one state could be resolved by Lindner et al. [34] which was attributed to an excitation into a 3p Rydberg state with E symmetry. Ishii and Hitchcock [36] assigned R_1 to a 3s type final state (similar to Prince et al. [29, 31]) and R_2 to an unoccupied state of the methyl group with π symmetry.

According to calculations (discussed at a later point in this manuscript), the C–O bond of methoxy on $V_2O_3(0001)$ is tilted by 57.4° with respect to the surface normal. This fits well to the moderate polarization dependence of all levels. The work of Lindner et al. [34] identifies (in agreement with the assignment of Ishii and Hitchcock [36]) R_3 as a C–O σ^* resonance. In a high symmetry environment this would mean that this resonance can only be excited by light with a component of the electric field vector pointing along the C–O bond. With this selection rule in mind one would probably expect that R_3 is more intense for $\alpha = 0°$ than for $\alpha = 80°$, in contrast to the experimental result (see Fig. 13). However, in the case of methoxy on $V_2O_3(0001)$ the local symmetry is not higher than Cs due to the tilted C–O bond. Therefore the selection rule is not as strict as in the high-symmetry case: for Cs symmetry the selection rule requires that the electric field vector has a component in the molecular plane. One may expect that the high-symmetry selection rule prevails if the distortion of the C–O σ^* level (induced by symmetry reduction) is only moderate, but a somewhat reliable quantitative statement regarding the polarization dependence of the R_3 intensity would require NEXAFS calculations which are not available at present. Since the same conclusion applies to the intensities of R_1 and R_2 we do not try the use their polarization dependence to discuss their assignment at this point. Nevertheless, we can clearly state that the observed moderate dependence of the NEXAFS

resonances on the light incidence angle is in full agreement with the result of the calculations which predict a strongly tilted geometry of the methoxy groups on $V_2O_3(0001)$.

4.3 Formation of Formaldehyde

Figure 14 shows TPD spectra obtained from a methanol adsorbate on an weakly reduced oxide layer containing ^{16}O and ^{18}O. In this case spectra obtained for mass 29 and mass 31 both show the signature of formaldehyde for all two formaldehyde desorption peaks demonstrating that formaldehyde molecules containing ^{18}O desorb from the surface. Since the adsorbed methanol molecules did not contain ^{18}O, an exchange of adsorbate oxygen atoms with substrate oxygen atoms must have occurred. This may be explained by assuming that formaldehyde forms via a dioxymethylene (O_2CH_2) intermediate as also proposed for methanol on chromia [37] and ceria [38] substrates. The CH_2 group would be coordinated to the substrate surface via two oxygen atoms, one being the oxygen atom of the methanol molecule and the other one being a substrate oxygen atom. Formaldehyde would form by cleavage of one of the C–O bonds and whether the formaldehyde finally contains substrate oxygen or methanol oxygen would depend on which bond is cleaved.

In the temperature range from 470 to 630 K also a considerable amount of methane is formed (see Fig. 11). Methane formation includes breaking of the C–O bond of the methoxy groups and bond formation to a surface hydrogen atom (net reaction: $CH_3O + H \rightarrow CH_4 + O$). It appears that a higher degree of surface reduction favors methane formation (compare Fig. 11a and b).

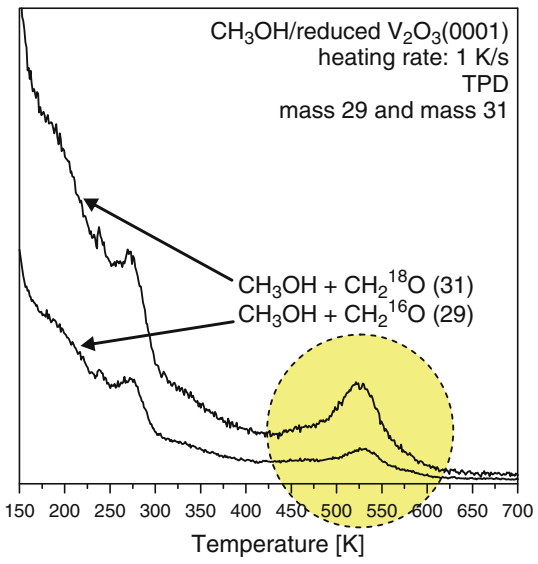

Fig. 14 Thermal desorption spectra (mass 29 and 31) of methanol on a weakly reduced oxide layer (electron dose: 8 mC) containing a mixture of ^{16}O and ^{18}O

For the fully reduced surface also a significant amount of methanol desorbs up to temperatures of about 550 K (see Fig. 11b). This shows that some of the hydroxy groups have not reacted to form water at 240 K. They are still on the surface above this temperature and may react with methoxy groups to form methanol which desorbs. Some water desorbs at about 515 K which also indicates that hydroxy groups are present. This is not unexpected since part of the hydroxy groups resulting from the fission of water molecules were shown to be stable on a reduced surface up to a temperature of $\sim$600 K [39]. Another source of hydrogen is the formation of formaldehyde which produces hydrogen atoms ($CH_3O \rightarrow CH_2O + H$).

The O–H vibration of adsorbed hydroxy groups can not be identified in Figs. 9 and 10 since there are spectrometer-related signals in the energy range of the O–H vibration which render the weak vibration unidentifiable. Since the spectrometer-related signals are similar in all spectra we divided the spectra shown in Figs. 9 and 10 by the spectra recorded after annealing at 600 K to reduce the spurious intensity (see Fig. 15). The data for the fully reduced surface in Fig. 15a clearly exhibit a rather broad absorption band centered around 3,625 cm^{-1} [which is near to the value of 3,641 cm^{-1} found by Abu Haija et al. [39] for hydroxy groups produced by water dissociation on

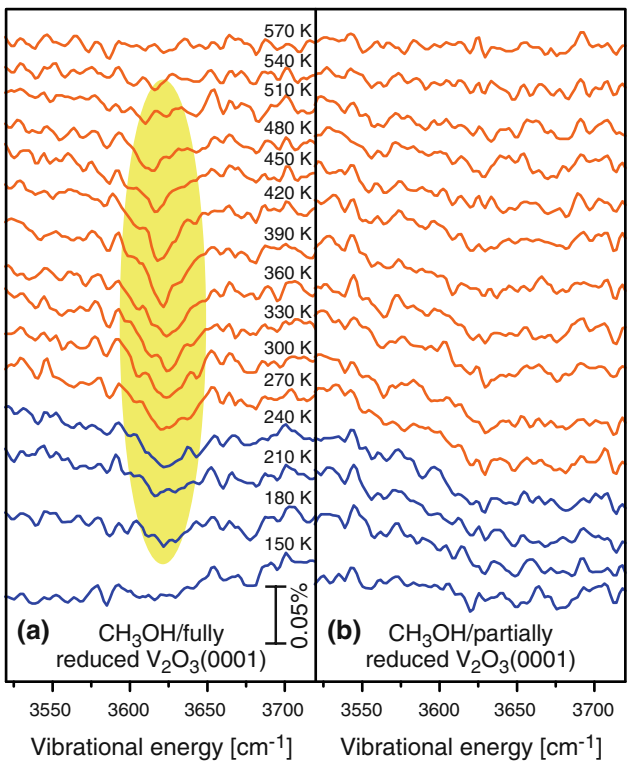

Fig. 15 Energy range of the O–H vibrations of part of the spectra shown in Figs. 9 and 10. To reduce spectrometer-induced signals in the relevant energy range the spectra were divided by the spectra recorded after annealing at 600 K. *Color code* as in Fig. 9

vanadium terminated $V_2O_3(0001)$] whereas there is only a very weak, somewhat questionable signal in the spectra shown in Fig. 15b which correlates well with the intensities of the methanol TPD signals in Fig. 11. The band in Fig. 15a appears to have an intensity maximum in the temperature range from 330 to 360 K. The corresponding infrared data in Fig. 10 show that this is about the temperature where the band of molecular methanol at 1,065 cm^{-1} vanishes which may be an indication that the low intensity of the O–H vibration at lower temperature is due to a hydrogen bridge–bond interaction between the OH groups and the methanol molecules as also indicated by DFT (see Sect. 5). That molecular methanol on the vanadium terminated surface may be stable even at 330 K is also indicated by the TPD data shown in Fig. 11b which exhibit a methanol desorption maximum at ~370 K. At higher temperature the intensity of the O–H vibrational band Fig. 15a vanishes due to methanol and water formation and no intensity increase is found when formaldehyde productions sets in which may be an indication that the hydroxy groups produced during formaldehyde production are only short-lived.

At ~490 K the rate of methanol desorption starts to drop and formaldehyde as well as methane production sets in (see Fig. 11b) which indicates that the hydroxy groups are now consumed for the production of methane instead for methanol formation (such a mechanism was also suggested by Farfan-Arribas for methanol on defective $TiO_2(110)$ [11]). The water desorption peak is rather small compared to the methane peak and hydrogen desorption is not observed at all which shows that most hydrogen atoms are consumed for the production of methane. This could also be the explanation for the identical desorption temperatures of methane and formaldehyde: as soon as hydrogen atoms are formed by abstraction from the methoxy groups they are consumed by other methoxy groups to form methane. However, in the case of the fully reduced surface hydrogen atoms are existent on the surface at temperatures below the formaldehyde formation temperature but methane is only formed at temperatures where also formaldehyde is produced which may be an indication that the rate limiting steps are the same for both reactions and that the outcome of the reaction (formaldehyde or methane) just depends on the availability of hydroxy groups.

The interaction of water with a partially reduced surface has not yet been investigated, but from the much weaker methanol desorption signal in Fig. 11a at temperatures above 325 K it may be concluded that the coverage of hydroxy groups surviving until this temperature is much smaller than in the case of the vanadium terminated surface. This is probably the reason why more formaldehyde and less methane is formed. The smaller density of hydroxy groups on the weakly reduced surface is a hint that the stability of hydroxy groups at elevated temperatures requires the existence of extended surface areas without vanadyl groups.

The discussion in the last paragraphs shows that the abundance of hydroxy groups at elevated temperature controls the selectivity of the oxide layer towards formaldehyde formation. If a reaction path which is more attractive than methane formation is offered to the hydroxy groups it may be expected that the amount of formaldehyde increases at the expense of the amount of methane. Such a handle to steer the selectivity of the reaction could for instance be the availability of weakly bound surface oxygen which means that a vanadium oxide with a higher oxygen content could exhibit a better selectivity towards formaldehyde but also a higher chance for further oxidation. Another ingredient in this discussion is probably the oxygen vacancy formation energy. If methoxy is transformed into methane then the oxygen atoms of the methoxy group will remain on the surface where it heals an oxygen vacancy. The higher the oxygen vacancy formation energy is the more methane formation is energetically favored. As shown in ref. [40] the vanadyl oxygen vacancy formation energy is 3.56 eV for $V_2O_3(0001)$ and 1.84 eV for $V_2O_5(001)$ which could mean that methane formation does not occur on $V_2O_5(001)$. Recent experiments for this system (data not shown here) support this conclusion.

5 Theoretical Considerations

5.1 Adsorption of Methanol

First we will look at the adsorption of methanol on the vanadyl terminated $V_2O_3(0001)$ surface. We use a 2×2 supercell with two vanadyl oxygen vacancies as model. Two molecules of methanol can adsorb molecularly with an adsorption energy of 0.94 eV per molecule (see Fig. 16a). Dissociative adsorption can occur by hydrogen transfer from the methanol hydroxy group to an adjacent vanadyl oxygen atom, creating a methoxy group at the vanadium defect site and a hydroxy group at the former vanadyl site. This type of adsorption is strongly favored over molecular adsorption; we find an adsorption energy of 1.86 eV per methanol molecule. With this type of adsorption a $V(OCH_3)$ and a V(OH) group are formed per defect. After dissociative adsorption the vanadium atoms at the defect sites are in a +4 oxidation state as compared to a 3+ state on the uncovered surface. The formation of V^{4+} is the driving force in the reaction. Vanadium atoms at vanadyl sites are V^{5+}.

In the experiments, the surface is subjected to an excess of methanol and we therefore consider the adsorption of four molecules on the defective surface. We find a structure

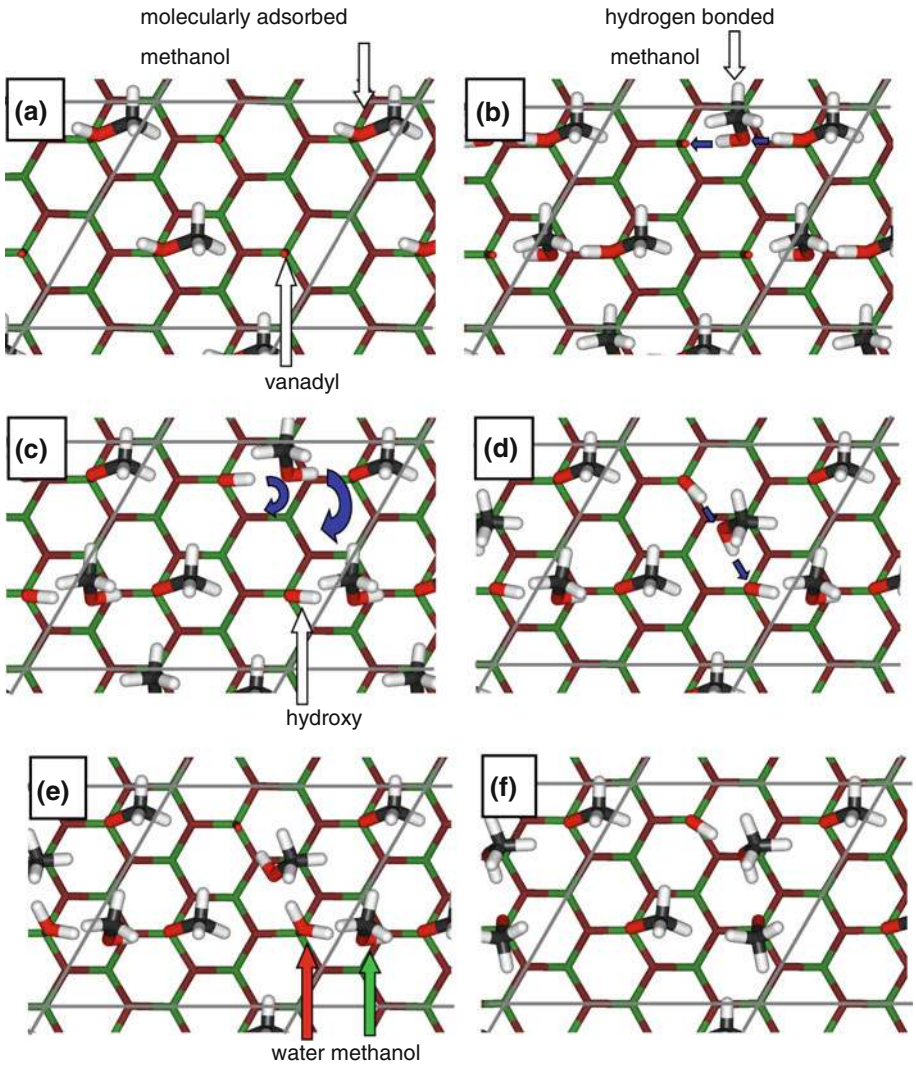

Fig. 16 DFT results for the adsorption of methanol on a partially reduced $V_2O_3(0001)$ surface. *Green* vanadium; *red* oxygen; *black* carbon; *light gray* hydrogen

with two methanol molecules molecularly adsorbed on the defects, and two additional molecules bound by hydrogen bonds (see Fig. 16b). The OH groups of the molecularly adsorbed molecules form hydrogen bonds to the oxygen atoms of the hydrogen bonded molecules, while the OH groups of these form hydrogen bonds to adjacent vanadyl oxygen atoms. The average adsorption energy per methanol molecule is 1.22 eV, even higher than that for the molecular adsorption, although two molecules only interact by hydrogen bonds, which can be explained by the strength of the hydrogen bonds—the structure is halfway to dissociative adsorption. The hydrogen bonded methanol molecules can mediate the dissociation by transfers of hydrogen atoms. The $V(HOCH_3)$ moiety transfers hydrogen to a hydrogen bonded methanol molecule and this transfers its hydroxy hydrogen atom to the vanadyl oxygen atom (indicated by blue arrows in Fig. 16b), yielding a methoxy and a hydroxy group, while retaining a hydrogen bonded methanol molecule (see Fig. 16c). As expected the reaction is exothermic (−0.42 eV). The barrier for such a shift reaction is probably small; we expect this reaction to occur even at low temperature. This is in line with the experimentally found decrease of vanadyl intensity after dosing methanol onto the surface at low temperature. The additional methanol molecules remain hydrogen bonded, and the interaction with the surface is quite strong. We find a desorption energy of 0.58 eV per molecule. Water formation starts with a rearrangement of one methanol molecule to a position between the two surface hydroxy groups (movement indicated by a blue arrow in Fig. 16c). This rearrangement is only slightly endothermic (0.03 eV, see structure in Fig. 16d). The methanol molecule can now mediate another hydrogen shift, forming a V=O and a $V(OH_2)$ species. This shift reaction is also slightly endothermic (0.15 eV, see structure in Fig. 16e). In the next step the water molecule (red arrow in Fig. 16e) is displaced by one of the additional methanol molecules (marked by a green arrow in Fig. 16e). The remaining hydrogen bonded

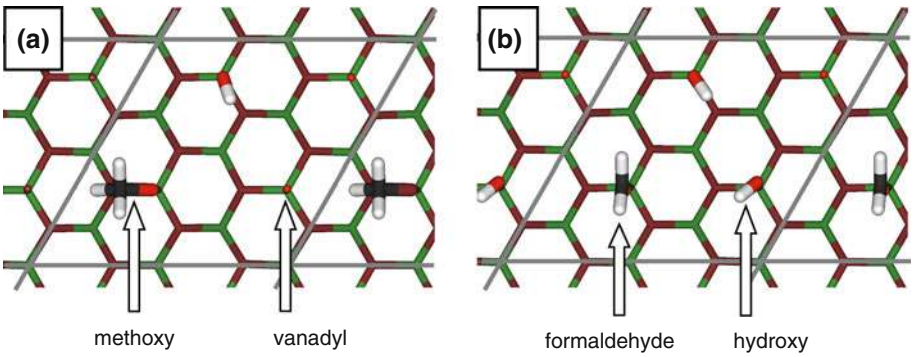

Fig. 17 DFT results for the oxidation of methanol on a partially reduced $V_2O_3(0001)$ surface

methanol mediates dissociation of this molecule by hydrogen transfer. This creates an additional methoxy and a hydroxy site (see Fig. 16f). We assume that the water leaves the surface at this step and that the sequence of reaction steps needs an elevated temperature because the steps are endothermic. The desorption of water produces a vanadyl oxygen vacancy which can serve as reactive center for further dissociative methanol adsorption, in agreement with the experimental findings. For a large number of defects this process would lead to a final state with twice as many methoxy groups than original defects. As indicated in Fig. 5, methoxy formation does also proceed when the sample is exposed to methanol at room temperature. In this case the surface coverage with molecular methanol is probably small so that methanol mediated hydrogen transfer is not a very likely process. This observation might thus indicate that at room temperature the O–H scission process can overcome the barrier for direct hydrogen transfer.

Identifying the water desorption energy as the energy difference between the state before hydroxy combination and the state after water desorption, we find a reaction energy of 0.69 eV, in good agreement with the experimental desorption energy of 0.74 eV as calculated with the Redhead equation [41] using an attempt frequency of $10^{13}s^{-1}$ and a desorption temperature of 270 K (see Fig. 6). In contrast to the experimental result, the calculated water desorption energy is higher than the calculated desorption energy of hydrogen bonded methanol (0.58 eV) for the structure shown in Fig. 16b, but our PBE calculations do not properly account for the dispersion term [42, 43], which will hardly change the water adsorption energy, but may increase the methanol adsorption energy by as much as 0.2 eV [44].

5.2 Oxidation of Methoxy Groups

To study the oxidation of methoxy groups we use again a 2×2 cell. In contrast to the study of adsorption we use a lower defect concentration of $\Theta = 0.25$ and consider a starting point with one surface methoxy, one hydroxy and two vanadyl sites. This choice should not be too far from the situation in the experiment. Furthermore the change of the model between adsorption and oxidation should not pose a problem, because the two reactions are well separated in the experiment; they occur in different temperature ranges. The energy for dissociative adsorption is slightly higher than above (2.0 vs. 1.86 eV, see Fig. 17a), but the difference is moderate and an increased adsorption energy at lower occupation is to be expected. In a previous study of methanol oxidation by silica supported vanadia [45], it was found that the oxidative step is hydrogen abstraction from the CH_3 group by a vanadyl oxygen, forming formaldehyde and VOH (see Fig. 17b). The same mechanism can occur on $V_2O_3(0001)$, if vanadyl groups are present after adsorption. We find a reaction energy of 1.46 eV for this oxidation step. This value is similar to the 1.79 eV obtained with PBE for silica supported vanadia using the structures optimized in ref. [45]. It is known that GGA functionals such as PBE used in the present work overestimate energies for the reduction of vanadia [46, 47] compared to the more reliable hybrid functional B3LYP. For silica supported vanadia the B3LYP value is 0.83 eV, but for the present case hybrid functional cannot be applied due to the high demand of computational resources. We can only state that the energy for the formation of formaldehyde is similar to that for silica supported vanadia. Although we have not calculated an energy barrier in this work, we assume that the barrier is comparable to silica supported vanadia, where a value of 1.42 eV was calculated [45].

6 Summary and Conclusions

We have investigated the adsorption of methanol on $V_2O_3(0001)$. Methanol does not react on vanadyl terminated $V_2O_3(0001)$; only molecular adsorption and desorption were found. If some or all oxygen atoms of the vanadyl groups are removed, methanol may dissociate on the surface already at low temperature (85 K) forming methoxy and hydroxy groups. In the case of a partial

removal of vanadyl oxygen, the hydrogen atoms may bind to vanadyl groups. The resulting hydroxy groups combine to form water at 270 K, producing vanadyl and vanadium sites. These may react with methanol to form more methoxy groups which finally leads to a methoxy density on the surface which is twice as high as the initial defect density. The DFT results essentially agree with the experimental findings and show that transfer of hydrogen via co-adsorbed methanol molecules is a critical mechanism for the formation of surface hydroxy groups and water.

Methoxy is also formed on fully reduced $V_2O_3(0001)$, but in this case vanadyl oxygen atoms are not available so that oxygen atoms from the $V_2O_3(0001)$ surface layer most likely bind the hydrogen atoms. Between 470 and 630 K two states of formaldehyde and methane desorption are found. We assume that the desorption state at lower temperature is due to formaldehyde formed in the presence of vanadyl groups whereas the high energy state is attributed to formaldehyde formed in an area of the surface where vanadyl oxygen atoms are not available.

In addition to formaldehyde also methane is formed and no reaction products remain on the surface after methane and formaldehyde desorption. This shows that the hydrogen atoms produced during formaldehyde production are consumed in the methane formation process. In the case of the fully reduced surface some hydrogen atoms produced in the course of the formation of the methoxy layer at low temperature are still on the surface when methane and formaldehyde formation sets in. Here more methane is formed which leads us to the conclusion that the abundance of hydrogen controls the selectivity of the surface for formaldehyde formation.

Acknowledgements This work was funded by the Deutsche Forschungsgemeinschaft through their Sonderforschungsbereich 546 'Transition Metal Oxide Aggregates'. The Fonds der Chemischen Industrie is gratefully acknowledged for financial support. We acknowledge the Helmholtz-Zentrum Berlin—Electron storage ring BESSY II for provision of synchrotron radiation at beamline UE52-PGM.

References

1. Grzybowska-Swierkosz B, Trifiro F, Vedrine JC (eds) (1997) Vanadia catalysts for selective oxidation of hydrocarbons and their derivatives. In: Applied catalysis A: general, vol 157. Elsevier, Amsterdam
2. Busca G, Lietti L, Ramis G, Berti F (1998) Appl Catal B 18:1
3. Cai Y, Ozkan US (1991) Appl Catal 78:241
4. Wachs IE (2005) Catal Today 100:79
5. Burcham LJ, Deo G, Gao X, Wachs IE (2000) Top Catal 11/12:85
6. Romanyshyn Y, Guimond S, Kuhlenbeck H, Kaya S, Blum RP, Niehus H, Shaikhutdinov S, Simic-Milosevic V, Nilius N, Freund H-J, Ganduglia-Pirovano MV, Fortrie R, Döbler J, Sauer J (2008) Top Catal 50:106
7. Wang Q, Madix RJ (2002) Surf Sci 496:51
8. Wong GS, Concepcion MR, Vohs JM (2002) J Phys Chem B 106:6451
9. Wong GS, Kragten DD, Vohs JM (2000) Surf Sci 452:L293
10. Wong GS, Kragten DD, Vohs JM (2001) J Phys Chem B 105:1366
11. Farfan-Arribas E, Madix RJ (2003) Surf Sci 544:241
12. Mullins DR, Robbins MD, Zhou J (2006) Surf Sci 600:1547
13. Dupuis A-C, Abu Haija M, Richter B, Kuhlenbeck H, Freund H-J (2003) Surf Sci 539:99
14. Feulner P, Menzel D (1980) J Vac Sci Technol 17:662
15. Abu Haija M, Guimond S, Romanyshyn Y, Uhl A, Kuhlenbeck H, Todorova TK, Ganduglia-Pirovano MV, Döbler J, Sauer J, Freund H-J (2006) Surf Sci 600:1497
16. Kresse G, Surnev S, Schoiswohl J, Netzer FP (2004) Surf Sci 555:118
17. Schoiswohl J, Sock M, Surnev S, Ramsey MG, Netzer FP, Kresse G, Andersen JN (2004) Surf Sci 555:101
18. Nilius N, Brázdová V, Ganduglia-Pirovano M-V, Simic-Milosevic V, Sauer J, Freund H-J (2009) New J Phys 11:093007
19. NIST chemistry WebBook. http://www.webbook.nist.gov/chemistry/
20. Pratt SJ, Escott DK, King DA (2003) J Chem Phys 119:10868
21. Bolina AS, Wolff AJ, Brown WA (2005) J Chem Phys 122:044713
22. Mudalige K, Trenary M (2002) Surf Sci 504:208
23. de Barros RB, Garcia AR, Ilharco LM (2003) Surf Sci 532:185
24. Andersson MP, Uvdal P, MacKerell AD Jr (2002) J Phys Chem B 106:5200
25. Crossley A, King DA (1977) Surf Sci 68:528
26. Crossley A, King DA (1980) Surf Sci 95:131
27. Linke R, Curulla D, Hopstaken MJP, Niemantsverdriet JW (2001) J Chem Phys 115:8209
28. Hammaker RM, Francis SA, Eischens RP (1965) Spectrochim Acta 21:1295
29. Prince KC, Richter R, de Simone M, Alagia M, Coreno M (2003) J Phys Chem A 107:1955
30. Plashkevych O, Privalov T, Ågren H, Carravetta V, Ruud K (2000) Chem Phys 260:11
31. Prince KC, Richter R, de Simone M, Coreno M (2002) Surf Rev Lett 9:159
32. Stöhr J, Outka DA, Baberschke K, Arvanitis D, Horsley JA (1987) Phys Rev B 36:2976
33. Stöhr J, Sette F, Johnson AL (1984) Phys Rev Lett 53:1684
34. Lindner Th, Somers J, Bradshaw AM, Kilcoyne ALD, Woodruff DP (1988) Surf Sci 203:333
35. Outka DA, Stöhr J, Madix RJ, Rotermund HH, Hermsmeier B, Solomon J (1987) Surf Sci 185:53
36. Ishii I, Hitchcock AP (1988) J Electron Spectrosc Relat Phenom 46:55
37. Mensch MW, Byrd CM, Cox DF (2003) Catal Today 85:279
38. Zhou J, Mullins DR (2006) Surf Sci 600:1540
39. Abu Haija M, Guimond S, Uhl A, Kuhlenbeck H, Freund H-J (2006) Surf Sci 600:1040
40. Göbke D, Romanyshyn Y, Guimond S, Sturm JM, Kuhlenbeck H, Döbler J, Reinhardt U, Ganduglia-Pirovano MV, Sauer J, Freund H-J (2009) Angew Chem Int Ed 48:3695
41. Redhead PA (1962) Vacuum 12:203
42. Grimme S (2006) J Comput Chem 27:1787
43. Kerber T, Sierka M, Sauer J (2008) J Comput Chem 29:2088
44. Svelle S, Tuma C, Rozanska X, Kerber T, Sauer J (2009) J Am Chem Soc 131:816
45. Döbler J, Pritzsche M, Sauer J (2005) J Am Chem Soc 127:10861
46. Sauer J, Döbler J (2004) Dalton Trans 19:3116
47. Rozanska X, Sauer J (2008) Int J Quantum Chem 108:2223